This is a repository copy of *Morphological divergence in giant fossil dormice*.

Title: Morphological divergence in giant fossil dormice

Authors: Jesse J. Hennekam[1], Roger B.J. Benson[2], Victoria L. Herridge[3], Nathan Jeffery[4], Enric Torres-Roig[5], Josep Antoni Alcover[6], Philip G. Cox[1,7]

Affiliations:
[1]Hull York Medical School, University of York, UK

[2]Department of Earth Sciences, University of Oxford, UK

[3]Natural History Museum, London, UK

[4]Department of Musculoskeletal & Ageing Science, Institute of Life Course & Medical Sciences, University of Liverpool, UK

[5]Departament de Dinàmica de la Terra i de l'Oceà, Facultat de Ciències de la Terra, Universitat de Barcelona, Barcelona, Spain

[6]Departament de Biodiversitat i Conservació, Institut Mediterrani d'Estudis Avançats (CSIC-UIB), Esporles, Mallorca, Spain

[7]Department of Archaeology, University of York, UK

Corresponding author: Jesse J. Hennekam

Address: PalaeoHub, University of York, Wentworth Way, York, YO10 5DD, UK

Email: jjh556@york.ac.uk

1   **Abstract**

2   Insular gigantism – evolutionary increases in body size from small-bodied mainland ancestors - is a

3   conceptually significant, but poorly studied, evolutionary phenomenon. Gigantism is widespread on

4   Mediterranean islands, particularly among fossil and extant dormice. These include an extant giant

5   population of *Eliomys quercinus* on Formentera, the giant Balearic genus †*Hypnomys* and the

6   exceptionally large †*Leithia melitensis* of Pleistocene Sicily. We quantified patterns of cranial and

7   mandibular shape and their relationships to head size (allometry) among mainland and insular

8   dormouse populations, asking to what extent the morphology of island giants is explained by

9   allometry. We find that gigantism in dormice is not simply an extrapolation of the allometric trajectory

10 of their mainland relatives. Instead, a large portion of their distinctive cranial and mandibular

11 morphology resulted from population- or species-specific evolutionary shape changes. Our findings

12 suggest that body size increases in insular giant dormice were accompanied by evolutionary divergence

13 of feeding adaptations. This complements other evidence of ecological divergence in these taxa, which

14 span predominantly faunivorous to herbivorous diets. Our findings suggest that insular gigantism

15 involves context-dependent phenotypic modifications, underscoring the highly distinctive nature of

16 island faunas.

17

18 Keywords

19 Insular Gigantism; Geometric morphometrics; Allometry; Island rule; *Leithia*; *Hypnomys*

20

21 **Introduction**

22 Insular gigantism is a widespread macroevolutionary pattern [1,2]. It occurred on many Mediterranean

23 islands throughout the Neogene and Quaternary, and is known among small mammals including

24 dormice, hamsters, murids, lagomorphs, shrews and moonrats [3-10]. Despite its prevalence, the

25 ecological drivers of insular gigantism are rather complex, with climate, island area, availability of

26   resources, and the presence of competitors and predators all proposed to play a part [2, 11-18].

27   Similarly, the morphological consequences of gigantism are not well understood, and it is not clear

28   whether giant island species have attained large size via similar evolutionary pathways. This raises the

29   possibility that insular gigantism does not represent a single well-defined process, but in fact reflects

30   the outcomes of evolution in a broad set of distinct ecological contexts.

31   Shape changes associated with increasing body size (allometry) are suggested to either result

32   from optimised functionality based on natural selection, or from constraints that impose fixed or

33   slowly-evolving allometric trajectories [19]. Allometric constraints will result in shared allometric

34   patterns ('common allometry') among related species, and provide an expectation that evolution will

35   proceed along lines of least evolutionary resistance (or "genetic lines of least evolutionary resistance")

36   [20], represented by a multivariate factor of the genetic or phenotypic variation [21] (but see [22]).

37   Deviation from these lines might be expected during adaptation to distinct ecological niches, resulting

38   in functional modification in shape and size. However, the evolvability of allometric relationships, and

39   therefore the ability of ecological adaptation to cause divergent patterns of phenotypic evolution, is

40   variable [23,24]: divergence from allometric trajectories may be common on long macroevolutionary

41   timescales but are rare on shorter timescales.

42   The Island Rule describes extensive variation in both shape and size [1], and suggests a graded

43   trend from gigantism in small mammals to dwarfism in larger species [13]. The evolutionary timescales

44   of adaptation to insularity are generally short [25], meaning that divergence from an ancestral

45   allometric trajectory may be difficult to realise [24]. Nevertheless, the exceptional increase in body size

46   associated with insular gigantism can result in unexpected morphologies, and evolutionary shifts to

47   novel ecologies in context of the island setting might also be a powerful driver of evolutionary changes

48   in morphology via functional adaptation.

49   Dormice (Gliridae) are potent exemplars of the evolutionary 'island effect' of body size

50   increase, having evolved extraordinary large sizes more frequently than other mammals –and on at

51   least eight different islands since the beginning of the Miocene [26,27]. Furthermore, giant dormice

52 are known from both the fossil record (e.g. *Hypnomys* spp. from the Balearic Islands and *Leithia* spp.

53 from Sicily and Malta) and an extant population of *Eliomys quercinus* on the island of Formentera [28].

54 Dormice therefore provide an ideal study system for addressing key questions regarding insular

55 gigantism.

56   The fossil giants *Hypnomys* and *Leithia* most likely evolved from a mainland ancestor related

57 to the genus *Eliomys* (Leithiinae) [29,30,31]. Previous studies uncovered craniomandibular differences

58 between extant *Eliomys* populations and fossil island genera [31-34]. The possibility that they were

59 more than simply enlarged forms of their mainland relatives is further supported by the change in

60 ecological niche displayed by the extant giant population on Formentera, which shows increased

61 faunivory in its diet [28]. Furthermore, the morphological features of the extinct island giants imply

62 alternative lifestyles such as increased terrestriality in *Hypnomys* [31] and herbivory in *Leithia* [32].

63   Here, the cranial and mandibular morphology in the extant giant *Eliomys quercinus* from

64 Formentera and the extinct giant genera *Leithia* and *Hypnomys* are investigated in the context of a

65 large dataset of non-giant dormouse skulls. *Eliomys quercinus* has a large geographic distribution

66 across Europe, including several populations on Mediterranean islands. Alongside fossil giants and the

67 extant giant population on Formentera, non-giant *E. quercinus* still display significant intraspecific size

68 variations. We aim to understand the transformation of cranial and mandibular form (size and shape)

69 in giant dormice by investigating the allometric trajectory of non-giant dormice. Characterisation of

70 the common allometric trajectory within *E. quercinus* populations enables us to distinguish between

71 morphological differences occurring due to size variations and those potentially related to other

72 factors. We ask to what extent the cranial and mandibular morphologies of island giant dormice are

73 predicted by extrapolation of the allometric trajectory for extant non-giant dormice, or whether

74 additional morphological variation occurs during evolution of giant size – possibly driven by island-

75 specific shifts in ecology.

76

77 **Material and Methods**

78 *Sample*

79 We analysed the skulls and mandibles of 63 adult specimens (fully erupted third molar) of the extant

80 species *Eliomys quercinus.* Specimens were from the collections of the Senckenberg Museum,

81 Frankfurt (SMF), the Muséum National d'Histoire Naturelle, Paris (MNHN) and the Natural History

82 Museum, London (NHMUK). Table S1 includes a full list of all extant specimens used in this study and

83 details of our μCT scanning methods are given in Appendix S1. Because only adult individuals were

84 analysed, our analyses (see below) describe patterns of static allometry.

85   Size variation in *Eliomys* was characterised among geographically separated extant

86 populations and in fossil giants. We used centroid size (the square root of the summed squared

87 distances between landmarks and the centroid [35]) derived from our landmark configurations as a

88 size proxy. Our subsequent analyses focused on quantifying allometry within a single species, *Eliomys*

89 *quercinus*, the closest living relative of insular giant dormice lineages [29,30,31]. Ideally, we would

90 compare extinct giant dormice with their specific mainland ancestor populations. However,

91 phylogenetic relationships among populations of *E. quercinus* are not currently known, let alone the

92 relationships of mainland populations with extinct island giants.

93   Fossil specimens of the insular species *Hypnomys onicensis, H. morpheus* and *Leithia melitensis*

94 were included in the analyses based on μCT models (Appendix S1), with small missing portions

95 reconstructed from photogrammetric models of other specimens. The fossil specimens include: a

96 composite reconstruction of the skull of *L. melitensis* based on specimens present at the Museo

97 Geologico Gemmellaro (mgupPS 78: 1-5)[32]; the reconstruction of an *L. melitensis* mandible located

98 at the Museo Universitario di Scienze Della Terra, Rome (MUST R2s26); a well preserved skull of *H.*

99 *morpheus* from Cova des Coral·loides (unnumbered specimen, under the responsibility of the Heritage

100 Authorities of the Consell Insular de Mallorca, Palma); and a mostly complete skull of the giant Balearic

101 dormouse *H. onicensis* in the collection of the Institut Mediterrani d'Estudis Avançats, Esporles,

102 Mallorca (IMEDEA 106855). Although this specimen is likely a sub-adult, based on size, dental wear

103 and the unfused skull sutures, it is the most complete skull available of this species.

104

Shape analyses of extant dormice

Anatomical landmarks were recorded from each cranium (42 landmarks) and mandible (19 landmarks) using Avizo Lite v9.2.0 (Thermo Fisher Scientific, Waltham, MA, USA). The *Arothron* package [36] was used to import the landmarks into R v3.5.3 [37]. We used 3D geometric morphometrics to characterize shape variation among extant populations of *E. quercinus* and extinct giants. Generalized Procrustes Analysis (GPA) was performed, translating the landmark coordinates to the origin, scaling to unit centroid size, and rotating them to a shared orientation, using a least squares criterion [38,39]. This analysis separates variation in size (centroid sizes) from variation in shape (Procrustes coordinates) so they can be treated as individual variables. A Principal Component Analysis (PCA) was performed using the geometric morphometric R package *Morpho* v2.6 [40], in order to evaluate the data in a lower dimensional space and identify the largest variances in shape within the dataset.

Allometry

Analysis of variance (ANOVA) was used to test the effect of size on adult shape variation (i.e. static allometry) in *E. quercinus* and the fossil giants. Using the procD.lm() function with 999 iterations in the R package *geomorph* v3.2.0 [41], the following linear model formula was evaluated: $shape \sim log10(size)$, in which size is represented by centroid size. This analysis asks what changes in cranial or mandibular shape are associated with changes in cranial or mandibular size. Our initial analyses included a categorical variable differentiating between non-giant and giant dormice for both the extant dataset (including the extant Formentera giants), as well as the complete dataset (including the fossil giants). When used as a covariate, $shape \sim log10(size) + giant$, this variable asks whether giant dormice show specific differences in skull shape compared to non-giant dormice; when used as an interaction term, $shape \sim log10(size) * giant,$ it asks whether the relationship between shape and size (i.e. its slope) differs between giant and non-giant dormice.

129   Subsequent analyses aimed to quantify the allometric signal among non-giant populations and

130   therefore used a more restricted sample, excluding giants. The independent effects of population

131   (defined by geographic location) and sex on shape were evaluated for non-giant *Eliomys* specimens

132   using the model: $shape \sim log10(size) + population + sex$ (Tables S2 and S3). We also asked

133   whether the effect of allometry varies among populations (Table S1) using the model formula:

134     $shape \sim log10(size) * population$. The significance of coefficients and interaction terms in these

135   models was assessed using ANOVA with permutation procedures.

136

137   *Predicted Shape Model*

138   The allometric relationship defined above can be used to evaluate the extent to which the morphology

139   of (giant) specimens is explained by their size. A multivariate regression for allometry $shape \sim size$

140   can be expressed as $Y = C + BX + E$ [42], in which Y is the shape vector, C is the intercept, B is

141   the vector of the regression coefficients for size and represents the angle of the slope of the

142   multivariate regression line, X represents centroid size, and E explains the error term. When using

143   Procrustes coordinates, the size component X can be evaluated as the difference between the centroid

144   size of each specimen and mean centroid size across all specimens. This procedure renders the

145   intercept term C redundant with the mean shape from Procrustes superimposition.

146   Our analyses of allometry among non-giant dormice demonstrated a small, but significant,

147   contribution of population (i.e. geographic location) to cranial and mandibular shape variation (Tables

148   S2 and S3). Therefore, we used the allometric relationships derived from the model

149     $shape \sim log10(size) + population$ among non-giant dormice for the allometric base model in the

150   subsequent analyses.

151

152   *Predicting shape from size.*

153   The base allometric model provides a predicted shape for each specimen based on its size. The

154   Procrustes coordinates of individual specimens can be projected on to an axis described by the vector

155   of size coefficients, B, from the multivariate regression [43]. This vector defines an axis in multivariate

156   space and is equivalent to the common allometric component (CAC) [44]. The orthogonal projection

157   of specimens onto this axis gives a regression (or CAC) score. The plot of regression score against size

158   provides a 2D representation of the allometric model. Shape residuals describe how the true shape of

159   each specimen differs from its predicted shape and are represented in the plot as the vertical (i.e.

160   shape) deviation of each specimen from the regression line.

161

162   *Predicting size from shape.*

163   The base allometric model can also be used to infer a 'predicted size' for each specimen based

164   on its shape (Procrustes coordinates). Predicted sizes identify whether the shape of a specific specimen

165   resembles that of a smaller or a larger specimen. They also allow us to infer a best-fit shape based on

166   predicted size, representing the shape a specimen would have if it only deviated from allometric

167   expectations by modification of the position on the allometry line (under the assumption that all shape

168   variation between specimens is associated with allometry).

169   Predicted sizes were inferred using a custom-written R function: predict.size() (Appendix S2).

170   This function uses the regression vector from the base allometric model to generate a series of

171   predicted shapes representing individuals of different sizes. These predicted shapes are calculated

172   using a 2 x n matrix in which the first row comprises the vector of intercept values and the second row

173   comprises the coefficients of size in the base allometric model. This was multiplied by an m x 2 matrix,

174   in which the first column consists solely of ones and the second column contains an ascending

175   sequence of size values of length m. Our predict.size() function by default sets the upper size limit to

176   1.5 times the size of the largest individual within the dataset. The resulting matrix is transformed to an

177   array based on the number of landmarks within the configuration and its dimensionality, creating a

178   dataset comprising a sequence of shape coordinate data associated with the allometric trajectory per

179   increment of size. This approach can be used to generate predicted sizes of external specimens that

180   were not included in the base allometric model, provided they are superimposed on the consensus

181   shape of this model.

182   The extent to which specimen shapes differ from the shapes predicted by allometry, given

183   their predicted sizes, provides a measure of the amount of shape difference between specimen shapes

184   and their deviation from allometric expectations (given actual sizes) that cannot be explained simply

185   by modification of position on the allometry line. It therefore allows us to quantify the amount of non-

186   allometric shape deviation exhibited by a specimen, which might, for example, reflect individual-,

187   population- or species-specific variation. This is calculated as the orthogonal projection of specimen

188   shapes on the regression vector. Our predict.size() function estimates this by evaluating the Procrustes

189   distances between the actual specimen shape and every proposed shape on the regression vector. The

190   proposed shape with the shortest Procrustes distances is the indicator for predicted size.

191   The relationship between predicted and actual size for each specimen was displayed

192   graphically via a 'predicted size versus actual size', or PSvAS, plot. This method is complementary to

193   existing allometric methods, and allows for the evaluation of the shape of individual specimens with

194   respect to the base allometric model. A line with intercept = 0 and slope = 1 on this plot represents

195   shapes with predicted sizes that match their actual sizes. This identity line divides the graph into two

196   sections, the lower-right indicating specimens with a centroid size exceeding the predicted centroid

197   size based on shape, and the upper-left including specimens with larger predicted sizes than the actual

198   centroid size.

199

200   *Application of PSvAS to the dormouse dataset*

201   The PSvAS method was used for analysing the shape of giant dormice, based on an allometric base

202   model including non-giant, extant *Eliomys quercinus* specimens. The fit of the fossil and extant giants

203   within the model was analysed to determine whether certain morphological features are in line with

204   the allometric predictions, or can be considered distinct characteristics for giants. Because the giant

205   dormice are considerably different in size and shape compared to non-giant *Eliomys*, including such

206   specimens will affect the GPA and therefore influence the inferred allometric component. Instead,

207   these specimens were superimposed to the consensus shape of the base model rather than being

208   included in the original GPA.

209

210   **Results**

211   *Shape variation in dormice*.

212   Principal component ordinations for both the cranial and mandibular dataset depict a clear signal

213   related to the distinctive morphology of giant species (Figure 1A,D). The first principal component is

214   correlated with size variation of extant, non-giant populations, with more positive values being

215   associated with larger individuals. The second principal component appears to distinguish between

216   extant (negative values) and fossil (positive values) giants. Overall, these patterns are more defined in

217   the cranial analyses.

218

219   *Size-shape relationships*

220   Our initial analyses of allometry demonstrate statistical significance for an independent variable

221   distinguishing between giant and non-giant dormice both when including only extant populations, and

222   for the complete dataset including fossil specimens (Tables S4 and S5). This indicates a role for non-

223   allometric shape variation during the origin of giant dormouse cranial and mandibular morphology.

224   The interaction term of this variable is non-significant for the extant dataset, but significant for the

225   complete dataset including fossil specimens. This indicates that the relationship between shape and

226   size among living and extinct giants from multiple islands is different to that among non-giant

227   populations (Figure 1B,E). Our subsequent analyses further interrogate and characterize these

228   differences.

229

230   *Allometric base model*

231   ANOVAs demonstrate statistically significant effects of size and population on the allometric

232   base models for both mandibular and cranial shape (Tables S2 and S3). The effect of sex (21 females;

233   24 males; 1 unknown) on mandibular and cranial shape is non-significant and sex was therefore was

234   excluded from further analyses (p = 0.188; p = 0.271). The interaction term between size and

235   population is also non-significant (mandible: p = 0.548; skull: p = 0.346), indicating that there is no

236   evidence for population-specific allometric effects in non-giant dormice. Thus, the best model is:

237    $shape \sim log10(size) + population$; which explains 53% of the total variation in both the

238   mandibular and cranial datasets (Tables S2 and S3). The PSvAS model was used to evaluate the shape

239   of giant dormice crania and mandibles with respect to this allometric model, based solely on non-giant

240   dormice (Figure 1C,F).

241

242   *Predicted Size versus Actual Size*

243   The PSvAS plots describe the relationship between the size of each specimen and its predicted

244   size based on shape in context of the allometric model (Figures 1C,F and 2). Giant specimens in these

245   graphs are located firmly below the identity line, indicating that their shapes resemble the crania and

246   mandibles of smaller individuals (Table S6). This effect is generally more pronounced for mandibles

247   than for crania (Figure 1). Furthermore, the larger fossil specimens deviate more from the identity line

248   compared to the extant giants from Formentera.

249

250   *Predicted and actual morphology of giant dormice*

251   Procrustes distances quantify the difference between the actual shape of giants and the

252   predicted shapes based on the allometric model (Table S6). Differences between giant shapes and

253   expectations under the allometric base model are relatively large (cranium: 0.07 – 0.18, mandible: 0.08

254   – 0.22), especially within the fossil genera *Hypnomys* and *Leithia*. These differences remain large even

255   when using the predicted (best fit) size given shape (Table S6; cranium: 0.07 – 0.13, mandible: 0.06 –

256   0.12), indicating that the actual morphology of giants is rather poorly predicted by the allometric

257   model, suggesting that giant dormouse cranial and mandibular morphologies originated via largely

258   non-allometric evolutionary processes.

259   Based on both their actual and predicted sizes, the crania of larger dormice are expected to

260   have upper incisors that curve more posteriorly, an inferiorly angled rostrum, an increased maximum

261   width of the zygomatic arch, and a relative narrowing of the auditory meatus (Figure 2). The predicted

262   relative narrowing of the auditory meatus is seen in the fossil taxa, but other aspects of the actual

263   shapes of the giants deviate from these predicted shapes: none show the predicted curvature in the

264   incisors, and the proposed inferior angle of the rostrum is only evident in *Leithia melitensis*. The

265   widening of the zygomatic arch is present within fossil giants, but is absent in the extant Formentera

266   giants. Furthermore, the zygomatic widening in the fossil giants is located much more anteriorly than

267   predicted.

268   Predicted mandibular morphology of giant dormice is also very different from their actual

269   shapes. The predicted shapes show a very narrow and antero-posteriorly elongated structure, whereas

270   the actual giants have robust mandibles, with the posterior part being greatly enlarged dorsoventrally.

271   Although the PSvAS graph implies a best-fit for giant mandibular shapes similar to that of non-giant

272   dormice, the large Procrustes distances between the fitted shape and the actual shape (Table S6)

273   indicate this is not the result of isometric scaling. Instead, the giants exhibit some unique

274   morphologies; e.g. distinct features in *L. melitensis* include a foreshortened and relatively straight

275   lower incisor, an exceptionally large and unperforated angular process, a posteriorly located anterior

276   margin of the masseteric ridge, and a vertically oriented coronoid process.

277   As the cranial and mandibular warps were created using the respective landmark

278   configurations, features not included in the configuration, such as the shape of the auditory bullae,

279   cannot be reliably assessed using the warped images. Figure S2 shows the positioning of the landmarks

280   on the giants with regards to their predicted shapes. The width of the zygomatic plate, visible in lateral

281   view, seems to increase with size in the fossil specimens. Furthermore, all giants appear to have a

282   sharply angled cranial vault. Lastly, we noticed a peculiar enlargement of the occipital condyle when

283   observing the µCT scan of *H. morpheus,* not seen in other specimens.

284

285   **Discussion**

286   Extant giant Formentera dormice and fossil giant specimens of Sicily and Mallorca show substantial

287   craniomandibular differences from their non-giant relatives (*Eliomys quercinus*; Figures 1 and S3). Only

288   a small portion of these morphological differences can be explained by the allometric trajectories of

289   non-giant populations. Insular giant dormice therefore diverge substantially from allometric

290   expectations. Additionally, we recognized that different species of giant dormice show distinctive

291   deviations from their predicted shapes.

292

293   *Predicting giant size and shape*

294   The cranial and mandibular morphologies of living and extinct island giants are different from those

295   expected under an allometric model. Allometry-related aspects of the shapes of these giants are

296   generally more similar to those of smaller dormice (although they also show substantial non-allometric

297   shape differences), and this effect is more pronounced for the mandible than for the cranium (Figure

298   1C,F). Although the craniomandibular shapes of giant dormice are more similar to smaller dormice

299   than expected, this does not imply isometric scaling; the actual fit of the giants within the model is

300   rather poor, and is worse for larger specimens (see Procrustes distances Table S6). Phylogenetically,

301   the fossil specimens are more separated from the base model, potentially explaining the poor fit of

302   these shapes within the model. The biologically implausible geometries that result from extrapolation

303   of the allometric model to giant sizes provide an alternative explanation. For example, the predicted

304   skull shape based on the cranial size of *L. melitensis* (log centroid size = 5.02) has an unrealistically

305   flexed cranial vault and occipital region, including a highly constricted foramen magnum. A similarly

306   unlikely morphology is evident for mandibular geometry, with the expected shape at the size of *L.*

307   *melitensis* (log centroid size = 4.11) being implausible owing to the very thin mediolateral width of the

308   bone. Interestingly, the morphologies of smaller giants (Formentera population and *Hypnomys*) are

309   not correctly predicted by the allometric base model either. These observations suggest that flattening

310   or truncation of the allometric trajectory occurs at large size in order to maintain biological

311   functionality.

312   Only part of the morphology of giant dormice can be explained by flattening of the allometric

313   trajectory — large differences are also evident in comparison to their expected shapes based on

314   (smaller) 'best fit' centroid sizes (Table S6; Figure 2). This indicates the presence of population-specific

315   morphological features within island giants, potentially reflecting adaptive variation due to island-

316   specific environmental conditions or ecological shifts. For example, the extant giant population of

317   Formentera is noticeably more faunivorous compared to other populations [28]. This suggests either

318   that insular body size increases have resulted in a dietary niche shift, or that a shift towards carnivory

319   reflects insular selective pressures on Formentera and is the driver of evolutionary increases in body

320   size. Although this is not the classic explanation of large body size in small mammals on islands [1], it

321   indicates that morphological variation among dormouse populations could represent allometry and

322   dietary (or other ecological) adaptations.

323

324   *Morphological traits of giant dormice*

325   Cranial morphology of island giants clearly deviates from the allometric expectations, even when

326   compared to their 'predicted sizes' (i.e. best-fit sizes to the line of allometry; Figure 2). The robust

327   rostrum and narrowing of the infraorbital foramen within all fossil giants are not predicted by the

328   allometric model at any cranial size. The model predicts the zygomatic arch in giants to become more

329   enlarged posteriorly. In reality, the arch does get more robust, but its maximum width is located much

330   more anteriorly. Larger dormice show a dorso-ventral flattening of the skull and changes to the

331   posterior part of the mandible, such as an elongated coronoid process and enlarged condylar and

332   angular processes. These are areas associated with masticatory muscle attachment [45], and their

333   modification suggests relative increases in molar bite force [46,47] or gape [48,49]. Multiple studies

334 have already shown that small changes in cranial and mandibular size and shape can affect mechanical

335 advantage and gape, both of which will impact the range of dietary items that can be processed. This

336 effect has been shown in a number of mammalian groups [50-53] but is particularly well-studied in

337 rodents [54-60]. The flattening of the skull is commonly seen in more rupicolous dormice [61],

338 although it may also be product of enlarged body size owing to negatively allometric scaling of brain

339 size [62] and craniofacial evolutionary allometry (CREA)[63]. This pattern, which is seen in many

340 mammalian groups, predicts relatively smaller braincases and longer rostra in larger species [64,65].

341

342 *Unique features of giant dormouse species*

343 Significant modifications to shape and size can result from evolutionary adaptation to novel ecologies,

344 including new diets [22]. We therefore interpret the unique morphological features identified in the

345 giant dormouse populations as reflecting specific ecological adaptations to insular settings. As well as

346 diverging from the non-giant allometric trajectory, giant dormice also differ morphologically from one

347 another. Such differences can be the result of various factors, including variation in ecosystem

348 composition, ecological niche occupation, as well as duration of isolation on islands. The introduction

349 of *Eliomys quercinus* to Formentera is thought to have occurred roughly 4000 years ago, whereas both

350 *Hypnomys* and *Leithia* were isolated for millions of years. Even though the morphology of Formentera

351 dormice does not resemble an intermediate shape between an average-sized *E. quercinus* and the

352 fossil giants, the differences in duration of isolation are substantial. Many population-specific aspects

353 of giant dormouse cranial, and especially mandibular, structure complement previous evidence of

354 divergent dietary and other ecological traits in these taxa.

355

356   *Formentera*

357 The Formentera dormice are the only extant giants and are morphologically different from the fossil

358 giants. It is the only giant population retaining a large infraorbital foramen. Furthermore, the

359 mandibular morphology of this population is characterised by a deep angular notch and relatively large

360   coronoid process, in contrast to the fossil giants. This enlarged coronoid results in a larger attachment

361   area for the temporalis muscle, suggesting an increased incisor bite force, which would be

362   advantageous for the extensive faunivorous behaviour observed within the Formentera population

363   [28]. Previous research has suggested that faunivory, more than other diets, places unique pressures

364   on rodents, driving greater morphological change [59,66]. However, this is not the case in the dormice

365   studied here, with the Formentera population resembling non-giant dormice more than the other

366   giants, based on the relatively short Procrustes distances of the best-fit in the PSvAS model (cranium

367   0.07; mandible 0.06) (Table S6).

368

369   *Hypnomys*

370   The *Hypnomys* material in our dataset is much more robust than other dormice, with the exception

371   of *Leithia melitensis.* The PSvAS model indicates that the morphology of this genus is substantially

372   different from extant dormice (cranium 0.10; mandible 0.08). The *H. onicensis* specimen examined

373   here is considered a subadult and is less robust than *H. morpheus.* The latter is characterised by

374   exceptionally pronounced occipital condyles. The robust morphology of the zygomatic area and

375   mandible in the two *Hypnomys* specimens indicates well developed masseteric musculature, which

376   suggests a diet including tough foods for this genus. A more abrasive plant-based diet has also been

377   suggested based on molar microwear [67].

378

379   *Leithia*

380   *Leithia melitensis* is the largest and most robust dormouse. *Hypnomys* and *Leithia* show similar

381   morphological modifications, although these are often more pronounced within *Leithia* [32]. This also

382   explains the relatively large Procrustes distances seen in the PSvAS model for this species (cranium

383   0.13; mandible 0.12). In particular, the width of the rostrum and the zygomatic plate is exceptional.

384   The mandible within this giant has very large angular and condylar processes. It is the only giant in

385   which there appears to be no fenestration of the angular process. However, the functional significance

386   of this fenestra is unknown. The coronoid is deflected less posteriorly, resulting in a more upright

387   position. The anterior margin of the masseteric ridge is positioned more posteriorly than in other

388   dormice and the incisor is relatively short and curves less superiorly. The cranial and mandibular

389   features seen in *L. melitensis*, in particular the exceptionally robust mandible, likely represent

390   adaptations to a herbivorous diet [68], possibly explaining its extraordinary size. In addition,

391   considerable variability in wear of the molar row is seen within the analysed fossil material of *L.*

392   *melitensis* (Figure S4), indicating a relatively abrasive diet against which the molars were used

393   extensively, also consistent with herbivory.

394

395   *Conclusion*

396   Multiple, independent dormice lineages achieved exceptional large size in insular habitats since the

397   end of the Messinian Salinity Crisis (5.33 Ma [69]). Extrapolation of common allometry as an

398   evolutionary line of least resistance on short timescales predicts that island giants could have highly

399   similar craniomandibular morphologies. Moreover, a graded trend to gigantism as proposed by the

400   island rule suggests that the importance of selective pressures within an ecosystem varies in a

401   predictable manner [13,14]. However, we find that the morphologies of giant dormice are not an

402   extrapolation along the allometric gradient of non-giant populations. This indicates that insular

403   gigantism may lead to a deviation from the otherwise strong allometric conservatism suggested to

404   exist in rodents [70]. Furthermore, the cranial and mandibular features of giant dormice contain a

405   prominent population-specific component, illustrating divergence and inherently non-predictable

406   adaptations to various different ecological niches, on different islands. These differences in the

407   evolutionary pathways of island giants may reflect differences in ecosystem composition among

408   islands and through geological time. Our findings have implications that extend beyond the study of

409   giant dormice, suggesting that island adaptation may commonly involve ecological shifts that are

410   unique and context-dependent, resulting in a high diversity of evolutionary responses to insular

411   habitats in mammals.

412

References

1. Foster JB. 1964 Evolution of mammals on islands. *Nature* 202, 234–235.

2. Van Valen L. 1973 Pattern and the balance of nature. *Evol. Theory* 49, 31–49.

3. Freudenthal M. 1972 *Deinogalerix koenigswaldi* nov. gen., nov. spec., a giant insectivore from the Neogene of Italy. *Scripta Geol.* 14, 1-19.

4. Freudenthal M. 1976 Rodent stratigraphy of some Miocene fissure fillings in Gargano (prov. Foggia, Italy. *Scripta Geol.* 37, 1–23.

438   5. Daams R, Freudenthal M. 1985 *Stertomys laticrestatus*, a new glirid (dormice, Rodentia) from

439   the insular fauna of Gargano (Prov. of Foggia, Italy). *Scripta Geol.* 77, 21–27.

440   6. Freudenthal M. 1985 Cricetidae (Rodentia) from the Neogene of Gargano (Prov. of Foggia,

441   Italy). *Scripta Geol.* 77, 29–74.

442   7. Mazza P. 1987 *Prolagus apricenicus* and *Prolagus imperialis*: two new Ochotonids

443   (Lagomorpha, Mammalia) of the Gargano (Southern Italy). *Boll. della Soc. Paleontol. Ital.* 26,

444   233–243.

445   8. Angelone C. 2007 Messinian *Prolagus* (Ochotonidae, Lagomorpha) of Italy. *Geobios* 40, 407–

446   421.

447   9. Quintana J, Köhler M, Moyà-Solà S. 2011 *Nuralagus rex*, gen. et sp. nov., an endemic insular

448   giant rabbit from the Neogene of Minorca (Balearic Islands, Spain). *J. Vert. Paleontol.* 31, 231–

449   240. doi: 10.1080/02724634.2011.550367.

450   10. Agustí J, Bover P, Alcover JA. 2012 A new genus of endemic cricetid (Mammalia, Rodentia)

451   from the late Neogene of Mallorca (Balearic Islands, Spain). *J. Vert. Palaeontol.* 32, 722-726.

452   11. Case, TJ. 1978 A general explanation for insular body size trends in terrestrial

453   vertebrates. *Ecology* 59, 1-18.

454   12. Heaney LR. 1978 Island area and body size of insular mammals: evidence from the tri-colored

455   squirrel (*Callosciurus prevosti*) of Southeast Asia. *Evolution* 32, 29-44.

456   13. Lomolino MV. 1985 Body size of mammals on islands: the island rule reexamined. *Am. Nat.*

457   125, 310-316.

458   14. Lomolino MV. 2005 Body size evolution in insular vertebrates: generality of the island rule. *J.*

459   *Biogeogr.* 32, 1683-1699.

460   15. McNab BK. 2010 Geographic and temporal correlations of mammalian size reconsidered: a

461   resource rule. *Oecologia* 164, 13-23.

462   16. van der Geer AA, Lyras GA, Lomolino MV, Palombo MR, Sax DF. 2013 Body size evolution of

463   palaeo-insular mammals: temporal variations and interspecific interactions. *J. Biogeogr.* 40,

464   1440-1450.

465   17. van der Geer AA. 2014 Parallel patterns and trends in functional structures in extinct island

466   mammals. *Integr. Zool.* 9, 167-182. doi: 10.1111/1749-4877.12066

467   18. Lomolino MV, van der Geer AA, Lyras GA, Palombo MR, Sax DF, Rozzi R. 2013 Of mice and

468   mammoths: generality and antiquity of the island rule. *J. Biogeogr.* 40, 1427-1439.

469   19. Pélabon C, Firmat C, Bolstad GH, Voje KL, Houle D, Cassara J, Le Rouzic A, Hansen TF. 2014

470   Evolution of morphological allometry. *Ann. NY Acad. Sci.* doi:10.1111/nyas.12470

471   20. Schluter D. 1996 Adaptive radiation along genetic lines of least resistance. *Evolution* 50, 1766–

472   1774. doi:10.2307/2410734

473   21. Marroig G, Cheverud JM. 2010 Size as a line of least resistance II: direct selection on size or

474   correlated response due to constraints? *Evolution: International Journal of Organic*

475   *Evolution*, *64*(5), 1470-1488. doi: 10.1111/j.1558-5646.2009.00920.x

476   22. Marroig G, Cheverud JM. 2001 A comparison of phenotypic variation and covariation patterns

477   and the role of phylogeny. Ecology, and ontogeny during cranial evolution of New World

478   monkeys. *Evolution* 55, 2576–2600. doi:10.1111/j.0014-3820.2001.tb00770.x

479   23. Huxley JS. 1932 Problems of relative growth. New York, NY: Dial Press.

480   24. Voje KJ, Hansen TF, Egset CK, Bolstad GH, Pélabon C. 2014 Allometric constraints and the

481   evolution of allometry. *Evolution* 68, 866–885. doi:10.1111/evo.12312

482   25. Lister AM. 1989 Red deer dwarfing on Jersey in the last interglacial. *Nature* 342, 539– 542.

483   26. van der Geer AA, Lyras GA, de Vos J, Dermitzakis M. 2010 *Evolution of Island Mammals:*

484   *Adaptation and Extinction of Placental Mammals on Islands*. Oxford, UK: Wiley-Blackwell

485   Publishing.

486   27. Palombo MR. 2018 Insular mammalian fauna dynamics and paleogeography: a lesson from the

487   western Mediterranean islands. *Integr. Zool.* 13, 2-20. doi: 10.1111/1749-4877.12275.

488   28. Kahmann H, Lau G. 1972 Der Gartenschläfer *Eliomys quercinus ophiusae* Thomas, 1925 von der

489   Pityuseninsel Formentera (Lebensführung). *Veröffentlichungen der zoologischen*

490   *Staatssammlung München* 16, 29-49.

491   29. Daams R, De Bruijn H. 1995 A classification of the Gliridae (Rodentia) on the basis of dental

492   morphology. *Hystrix*, 6 (1-2), 3-50.

493   30. Freudenthal M, Martín-Suárez E. 2013 New ideas on the systematics of Gliridae (Rodentia,

494   Mammalia). [Nuevas ideas sobre la sistemática de Gliridae (Rodentia, Mammalia)]. *Spanish J.*

495   *Palaeont.* 28 (2), 239-252.

496   31. Bover P, Alcover JA, Michaux JJ, Hautier L, Hutterer R. 2010 Body shape and life style of the

497   extinct Balearic dormouse *Hypnomys* (Rodentia, Gliridae): new evidence from the study of

498   associated skeletons. *PLoS ONE* 5, e15817.

499   32. Hennekam JJ, Herridge VL, Costeur L, Di Patti C, Cox PG. 2020 Virtual cranial reconstruction of

500   the endemic gigantic dormouse *Leithia melitensis* (Rodentia, Gliridae) from Poggio Schinaldo,

501   Sicily. *Open Quat.* 6(1), 7. doi: http://doi.org/10.5334/oq.79

502   33. Orlandi-Oliveras G, Jordana X, Moncunill-Solé B, Köhler M. 2016 Bone histology of the giant

503   fossil dormouse *Hypnomys onicensis* (Gliridae, Rodentia) from Balearic Islands. *C R Palevol* 15,

504   238-244.

505   34. Mills DH. 1976 Osteological study of the Pleistocene dormouse *Hypnomus morpheus* Bate from

506   Mallorca (Rodentia, Gliridae). *Publ. Paleontol. Inst. Univ. Uppsala* 4, 5-73.

507   35. Zelditch ML, Swiderski DL, Sheets HD. 2012 *Geometric morphometrics for biologists: a primer*.

508   academic press.

509   36. Profico A, Veneziano A, Melchionna M, Raia P. 2018 Arothron: R functions for geometric

510   morphometric analyses. R package version 1.0.0, https://cran.r-

511   project.org/web/packages/Arothron/index.html

512   37. R Core Team, 2019. *R: A language and environment for statistical computing*. Vienna, Austria:

513   R Foundation for Statistical Computing.

514   38. Rohlf FJ. 1990 Morphometrics. *Ann. Rev. Ecol. Syst.* 21, 299–316.

515   39. Mitteroecker P, Gunz P. 2009 Advances in geometric morphometrics. *J. Evol. Biol.* 36, 235–247.

516   doi: 10.1007/s11692-009-9055-x.

517 40. Schlager S. 2017 Morpho and Rvcg – shape analysis in R. In *Statistical Shape and Deformation*

518   *Analysis* (eds G Zheng, S Li, GJ Székely), pp. 217–256. San Diego, CA: Academic Press.

519 41. Adams DC, Collyer ML, Kaliontzopoulo, A. 2018 Geomorph: Software for geometric

520   morphometric analyses. R package version 3.0.6. https://cran.r-

521   project.org/package=geomorph.

522 42. Klingenberg CP. 2016 Size, shape, and form: concepts of allometry in geometric

523   morphometrics. *Dev. Genes Evol.* 226, 113-137.

524 43. Drake AG, Klingenberg CP. 2007 The pace of morphological change: historical transformation

525   of skull shape in St Bernard dogs. *Proc. R. Soc. B* 275, 71-76.

526 44. Mitteroecker P, Gunz P, Bernhard M, Schaefer K, Bookstein FL. 2004 Comparison of cranial

527   ontogenetic trajectories among great apes and humans. *J. Human Evol.* 46, 679-698. doi:

528   10.1016/j.jhevol.2004.03.006.

529 45. Cox PG, Jeffery N. 2015 The muscles of mastication in rodents and the function of the medial

530   pterygoid. In *Evolution of the rodents: advances in phylogeny, functional morphology and*

531   *development* (eds PG Cox, L Hautier), pp. 350-372. Cambridge, UK: Cambridge University Press.

532 46. Hiiemae KM. 1971 The structure and function of jaw muscles in the rat (*Rattus norvegicus* L.)

533   III. The mechanics of the muscles. *Zool. J. Linn. Soc.* 50, 111-132.

534 47. Weijs WA, Dantuma R. 1975 Electromyography and mechanics of mastication in the albino rat.

535   *J. Morphol.* 146, 1-33.

536 48. Vinyard CJ, Payseur BA. 2008 Of "mice" and mammals: utilizing classical inbred mice to study

537   the genetic architecture of function and performance in mammals. *Integr. Comp. Biol.* 48, 324-

538   337.

539 49. Cornette R, Herrel A, Cosson J-F, Poitevin F, Baylac M. 2012 Rapid morpho-functional changes

540   among insular populations of the greater white-toothed shrew. *Biol. J. Linn. Soc. 107*, 322–331.

541 50. McIntosh AF, Cox PG. 2016 Functional implications of craniomandibular morphology in African

542   mole-rats (Rodentia: Bathyergidae). *Biol. J. Linn. Soc.* 117, 447-462.

543   51. Kiltie RA. 1982 Bite force as a basis for niche differentiation between rain forest peccaries

544   (*Tayassu tajacu* and *T. pecari*). *Biotropica* 14, 188-195.

545   52. Herrel A, McBrayer LD, Larsen PM. 2007 Functional basis for sexual differences in bite force in

546   the lizard *Anolis carolinensis*. *Biol. J. Linn. Soc.* 91, 111–119. doi: 10.1111/j.1095-

547   8312.2007.00772.x

548   53. Herrel A, de Smet A, Aguirre LF, Aerts P. 2008 Morphological and mechanical determinants of

549   bite force in bats: do muscles matter? *J. Exp. Biol.* 211, 86-91. doi: 10.1242/jeb.012211

550   54. Williams SH, Peiffer E, Ford S. 2009 Gape and bite force in the rodents *Onychomys leucogaster*

551   and *Peromyscus maniculatus*: Does jaw-muscle anatomy predict performance? *J.*

552   *Morphol.* 270, 1338-1347.

553   55. Cox PG, Rayfield EJ, Fagan MJ, Herrel A, Pataky TC, Jeffery N. 2012 Functional evolution of the

554   feeding system in rodents. *PLoS ONE* 7, e36299. doi: 10.1371/journal.pone.0036299.

555   56. Renaud S, Gomes Rodrigues HG, Ledevin R, Pisanu B, Chapuis J-L, Hardouin EA. 2015 Fast

556   evolutionary response of house mice to anthropogenic disturbance on a Sub-Antarctic island.

557   *Biol. J. Linn. Soc.* 114, 513–526.

558   57. McIntosh AF, Cox PG. 2016 Functional implications of craniomandibular morphology in African

559   mole-rats (Rodentia: Bathyergidae). *Biol. J. Linn. Soc*. 117, 447–462.

560   58. Cox, PG, Morris PJR, Hennekam JJ, Kitchener AC. 2020 Morphological and functional variation

561   between isolated populations of British red squirrels. *J. Zool.* doi: 10.1111/jzo.12829

562   59. Fabre P-H, Herrel A, Fitriana Y, Meslin L, Hautier L. (2017). Masticatory muscle architecture in

563   a water-rat from Australasia (Murinae, Hydromys) and its implication for the evolution of

564   carnivory in rodents. *J. Anat.* 231(3), 380-397.

565   60. Ginot S, Herrel A, Claude J, Hautier L. 2018 Skull size and biomechanics are good estimators of

566   in vivo bite force in murid rodents. *Anat. Rec.* 301, 256-266*.*

567   61. Holden-Musser ME, Juškaitis R, Musser GM. 2016 Gliridae. In *Handbook of the Mammals of*

568   *the World. Volume 6: Lagomorphs and Rodents I* (eds DE Wilson, TE Lacher, RA Mittermeier),

569   pp. 838-889. Barcelona, Spain: Lynx Edicions.

570 62. Penrose F, Kemp GJ, Jeffery N. 2016 Scaling and accommodation of jaw adductor muscles in

571   Canidae. *Anat. Rec.* 299, 951-966.

572 63. Cardini A, Polly D, Dawson R, Milne N. 2015 Why the long face? Kangaroos and wallabies follow

573   the same 'rule' of cranial evolutionary allometry (CREA) as placentals. *J. Evol. Biol.* 42(2), 169–

574   176. doi: 10.1007/s11692-015-9308-9

575 64. Radinsky LB. 1985 Approaches in evolutionary morphology: A search for patterns. *Annu Rev*

576   *Ecol Evol Syst.* 16(1), 1–14. https://doi.org/10.1146/annurev.es.16.110185.000245

577 65. Cardini, A. 2019 Craniofacial allometry is a rule in evolutionary radiations of placentals. *J. Evol.*

578   *Biol.* 46(3), 239-248.

579 66. Maestri R, Patterson BD, Fornel R, Monteiro LR, De Freitas TRO. 2016 Diet, bite force and skull

580   morphology in the generalist rodent morphotype. *J. Evol. Biol.*, 29(11), 2191-2204.

581 67. Hautier L, Bover P, Alcover JA, Michaux J. 2009 Mandible morphometrics, dental microwear

582   pattern, and paleobiology of the extinct Balearic dormouse *Hypnomys morpheus*. *Acta*

583   *Palaeontol. Pol.* 54, 181-194.

584 68. Michaux J, Chevret P, Renaud S. 2007 Morphological diversity of Old World rats and mice

585   (Rodentia, Muridae) mandible in relation with phylogeny and adaptation. *J. Zool. Syst. Evol.*

586   *Res.* 45, 263-279.

587 69. Krijgsman W, Hilgen FJ, Raffi I, Sierro FJ, Wilson DS. 1999 Chronology, causes and progression

588   of the Messinian salinity crisis. *Nature*, 400(6745), 652-655.

589 70. Wilson LA. 2013 Allometric disparity in rodent evolution. *Ecol. Evol.* 3, 971-984.
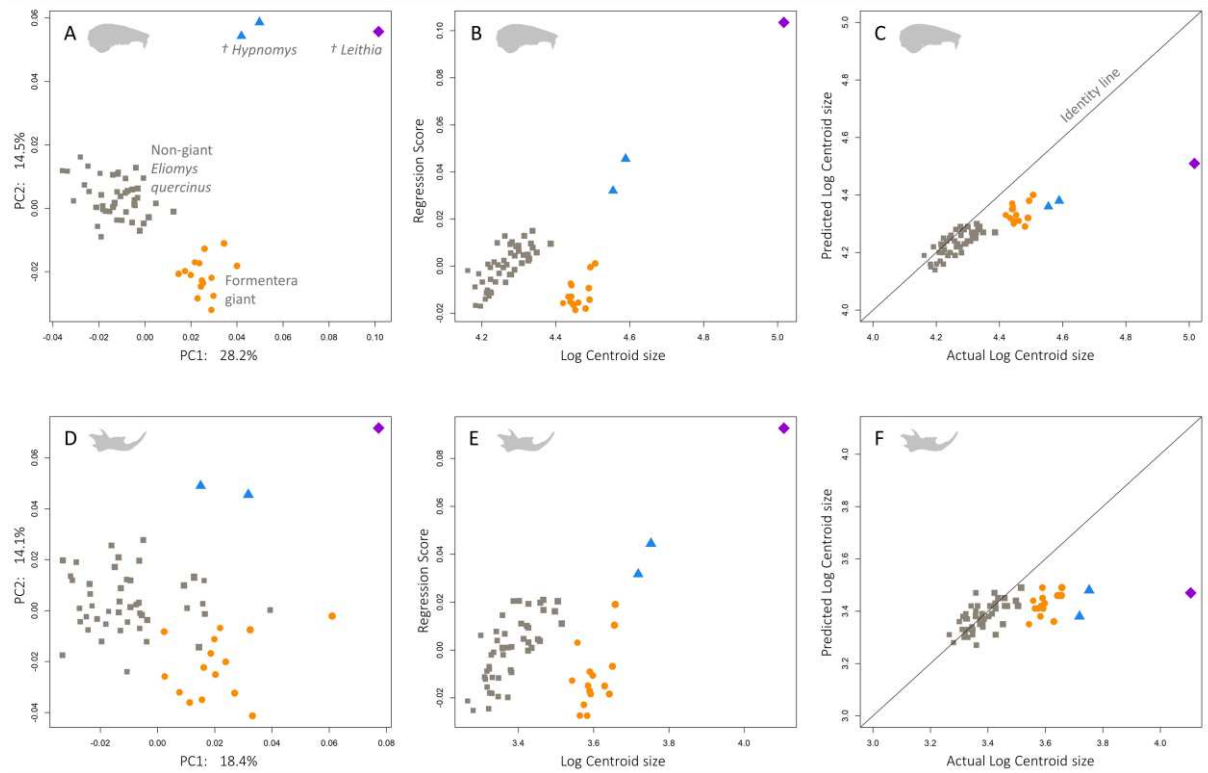
590

591

592

593

594

595

596 Figure 1:   Cranial (top) and mandibular (bottom) shape differentiation in extant *Eliomys quercinus*

597 specimens and fossil giants on the first two principal components (A,D); the common allometric

598 component versus log centroid size with grouping (B,E); and the predicted size versus actual size

599 analyses based on a non-giant base model including the predicted sizes for the giant Formentera

600 population and fossil giants (C,F).

601

602

603

604

605

606

607

608

609
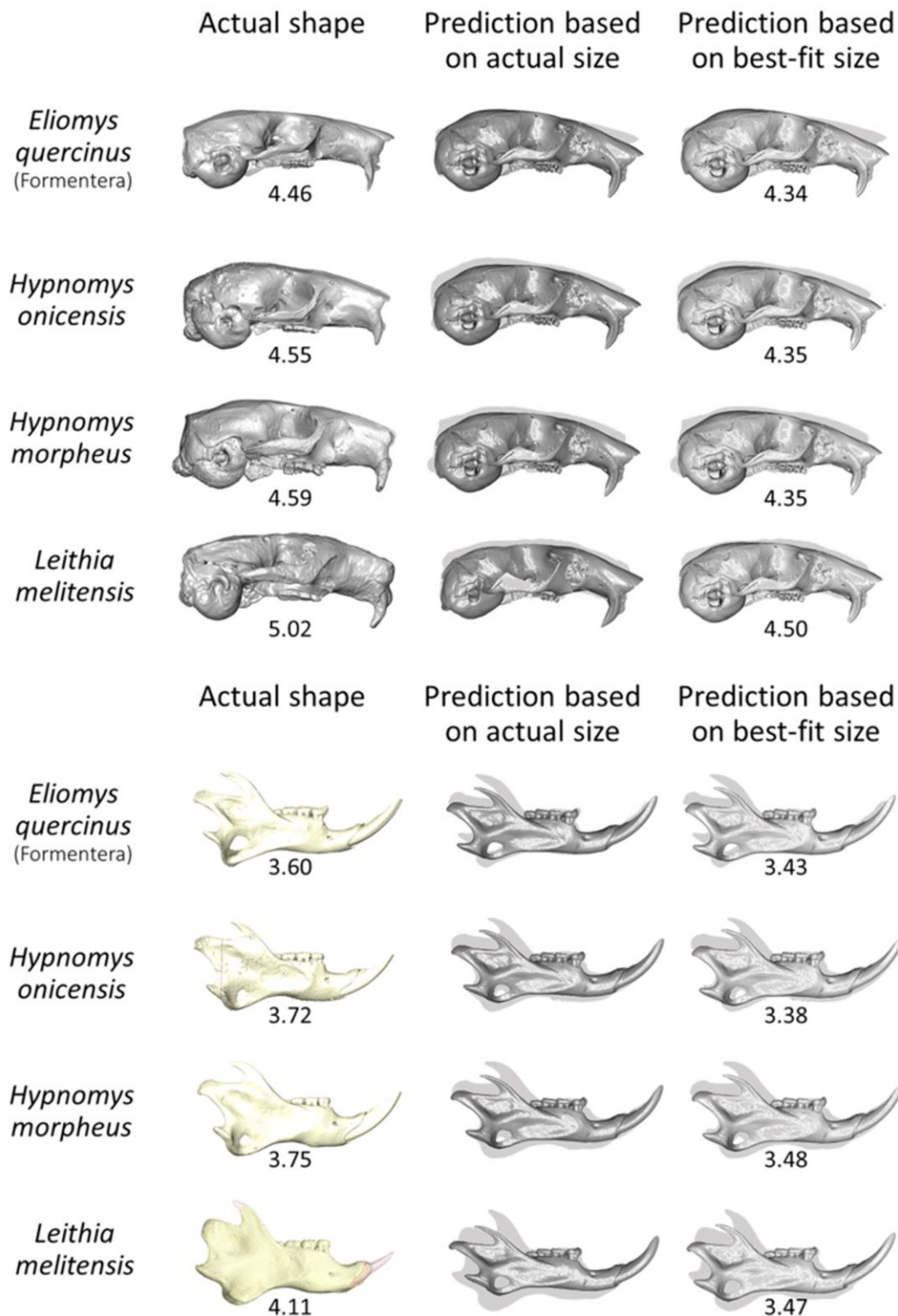
Figure 2: Predicted shapes of the fossil giants derived from the PSvAS model, using the shape predicted by the actual centroid size of the specimen and the shape presumed to be the best fit with the actual shape of the specimen.